

## Characterization of stickiness by means of recurrence

Yong Zou

*Nonlinear Dynamics Group, University of Potsdam, Am Neuen Palais 10, 14469 Potsdam, Germany*

Marco Thiel and M. Carmen Romano

*Department of Physics, University of Aberdeen, Aberdeen AB 24 3UE, United Kingdom*

Jürgen Kurths

*Nonlinear Dynamics Group, University of Potsdam, Am Neuen Palais 10, 14469 Potsdam, Germany*

(Received 27 April 2007; accepted 26 August 2007; published online 12 October 2007)

We propose recurrence plots (RPs) to characterize the stickiness of a typical area-preserving map with coexisting chaotic and regular orbits. The difference of the recurrence properties between quasiperiodic and chaotic orbits is revisited, which helps to understand the complex patterns of the corresponding RPs. Moreover, several measures from the recurrence quantification analysis are used to quantify these patterns. Among these measures, the recurrence rate, quantifying the percentage of black points in the plot, is applied to characterize the stickiness of a typical chaotic orbit. The advantage of the recurrence based method in comparison to other standard techniques is that it is possible to distinguish between quasiperiodic and chaotic orbits that are temporarily trapped in a sticky domain, from very short trajectories. © 2007 American Institute of Physics.

[DOI: [10.1063/1.2785159](https://doi.org/10.1063/1.2785159)]

**It is important to recognize that nonintegrable Hamiltonian systems exhibit chaos with some particular features; e.g., the full space is a complicated mixture of periodic, quasiperiodic, and chaotic orbits. A typical chaotic trajectory spends a long time near the border of stable islands, showing almost regular motion, which is a behavior called stickiness. The presence of stickiness causes some substantial difficulties in the use of conventional tools to characterize the dynamics when only short trajectories are available. In this paper, we present a careful numerical investigation of the recurrence properties of orbits from nonintegrable Hamiltonian systems by using a two-dimensional visualization technique: the recurrence plot (RP). We find that the patterns in the RPs of quasiperiodic and chaotic orbits are qualitatively different. These differences in the RPs allow distinguishing between regular and chaotic orbits that are temporarily trapped in a sticky domain in short trajectories. Furthermore, applying recurrence quantification analysis it is possible to understand these recurrence patterns quantitatively.**

### I. INTRODUCTION

It is well known that the phase space of a nonintegrable Hamiltonian system is neither entirely regular nor entirely chaotic. The whole phase space is a complicated mixture of domains of chaotic trajectories coexisting with domains of regular or periodic ones. In other words, the full space is decomposed into subregions associated with qualitatively distinct dynamical properties.<sup>1</sup> The regular dynamics consists of quasiperiodic orbits lying on tori and periodic orbits, while chaotic orbits are expected to fill the corresponding subspace densely.<sup>2</sup> In the case of two-dimensional area-preserving maps, invariant circles separate the phase space,

preventing trajectories in the chaotic sea from entering any island, and regular trajectories inside an island from reaching the chaotic sea. Hence, the characterization of orbits as regular or chaotic is crucial and it has attracted much attention.

In the literature, a frequently used method for this problem is the estimation of Lyapunov exponents. This measure is well justified and standard for the characterization of the nature of orbits. Chaotic motion is characterized by a positive Lyapunov exponent (in the case of the area-preserving maps, the sum of all exponents is zero). Regular orbits, on the other hand, have zero Lyapunov exponents. However, when resorting to numerical calculations, only a finite time is used, producing the so-called local (or finite-time) Lyapunov exponent. This is, of course, more important when dealing with experimental data, because of the rather small number of measurements. Calculations of finite-time Lyapunov exponents in Hamiltonian systems were performed in Ref. 3. It seems to be impossible to include all other methods and their associated developments reported in the literature as it is a fast growing field. For a review of such methods, see Ref. 4. Therefore, we only mention one popular approach in this spirit: the spectra of stretching numbers (or local Lyapunov exponents for only *one* iteration time), which have been shown to be efficient in distinguishing chaotic from regular trajectories.<sup>4-6</sup>

When the previous measures are applied, considerable attention is paid to the corresponding convergence rate, as it ensures a reliable characterization. This is particularly important for Hamiltonian systems with mixed phase space which are divided into different ergodic components. The dynamics inside each of these components might be regular (periodic or quasiperiodic) or chaotic. However, due to the existence of stable islands, a typical chaotic trajectory will need a long time to fill its corresponding component in phase space. In

particular, once the chaotic orbit is close to an island, it will stay close to it and will be almost regular in its motion for a rather long time. After this transient period, it escapes to the large chaotic sea. Such a long-term confinement of the trajectory in this domain is called stickiness.<sup>7,8</sup> Stickiness delays the convergence and might also cause some substantial difficulties in the use of Lyapunov exponents and the spectrum of stretching numbers. Therefore, characterizing a chaotic orbit reliably requires much computational effort. In some sense, it is reasonable to define a temporarily “sticky” chaotic orbit on time scales when it is stuck, respectively, a “filling” chaotic orbit on time scales when it travels unimpeded throughout the chaotic region.<sup>9</sup> This classification is rather useful for one carefully chosen chaotic orbit, which has a strong sticking time.<sup>5</sup> Note these two different and *relative* concepts coincide in the limit of long time when referring to one chaotic orbit.

The origin of the stickiness does not have a universal scenario. One mechanism that generates stickiness is by means of cantori, consisting of sets of destroyed tori, which serve as partial barriers. The orbits can cross a cantorus, albeit after a long time.<sup>8</sup> Islands-around-islands scenarios were reported in Refs. 10 and 11. Other simple mechanisms of stickiness cannot be excluded, such as the existence of one single marginal unstable fixed point,<sup>12</sup> or one-parameter families of marginal unstable periodic orbits in the phase space.<sup>13</sup> The first known example of stickiness was presented in Ref. 14. Nowadays, it has been accepted as a fundamental property of Hamiltonian systems. Stickiness may produce anomalous transport, which perhaps is the most prominent consequence.<sup>11</sup>

In this paper, we propose using recurrence plots (RPs) to characterize stickiness. We use the standard map, a two-dimensional area-preserving map, as an example. We follow the idea of Ref. 9 and categorize the trajectories into quasiperiodic, sticky, and filling chaotic orbits. Note that the stickiness is a general property of Hamiltonian chaos. Hence, the concept of sticky orbit only refers to the particular time scale when it is stuck. However, the use of this concept makes it convenient for us to compare the differences between these orbits and refer to the results of Refs. 5 and 6. As the name suggests, RPs concentrate on the recurrence properties of the orbits. As a result, a two-dimensional black-white plot (introduced in Sec. III) can be used to visualize the difference between quasiperiodic and sticky orbits. One popular method to characterize stickiness uses the distribution  $P(T)$  of the recurrence times  $\{T_1, T_2, \dots, T_M, \dots\}$  of a typical chaotic orbit to a predefined recurrence region. The stickiness is quantified in terms of an asymptotic power-law decay  $P(T) \sim T^{-\gamma}$  for large  $T$ , where  $\gamma$  is a scaling exponent.<sup>11,15</sup> This power-law can be related to the decay of the correlation function, survival probability and transport properties.<sup>11</sup> The recurrence quantification analysis (RQA), which is based on RPs, can also characterize the stickiness in a similar way.

The outline of the paper is as follows. In Sec. II the recurrence properties of quasiperiodic orbits to a predefined interval are reviewed. In Sec. III, we apply RPs to visualize the differences between ordered and chaotic orbits. The RQA

measures are used to quantify the patterns in the RPs in Sec. IV. Furthermore, in Sec. V we follow a typical chaotic orbit and use RQA to quantify its stickiness.

## II. RECURRENCES OF QUASIPERIODIC AND CHAOTIC ORBITS

We consider the standard map, which is a paradigmatic example of an autonomous near-integrable system with two degrees of freedom:

$$\vec{v}(t): \begin{cases} y_{n+1} = y_n + \frac{\kappa}{2\pi} \sin(2\pi x_n), \\ x_{n+1} = x_n + y_{n+1}, \end{cases} \quad \text{mod } 1 \quad (1)$$

with  $\kappa$  denoting a nonlinearity parameter. This model is probably the best-studied chaotic Hamiltonian map.<sup>1</sup> It can be interpreted as the a Poincaré section of a periodically kicked rotor. It also approximates other physical situations, such as the Fermi accelerator model.

For small nonlinearity parameters  $\kappa$ , those tori with a Diophantine rotation number, i.e.,  $\Omega \in \{\Omega: |n\Omega - m| > c/n^\tau, \forall m, n \in \mathbb{Z}, n \neq 0\}$  for some  $\tau > 1$  and  $c > 0$ , survive.<sup>10</sup> The onset of chaos is connected to the destruction of tori, i.e., the change of tori into cantori, as the perturbation increases. As a consequence, chaotic and regular trajectories are intimately intermingled. The Kolmogorov-Arnold-Moser (KAM) surfaces isolate the layers of stochasticity from each other and the stochastic excursions are constrained by nearby KAM curves.

The simple but little-known result of Slater’s theorem<sup>16</sup> allows detecting quasiperiodicity rather easily. This theorem states that for *any* irrational linear rotation with rotation number  $\Omega$  and for *any* connected interval of size  $\epsilon$ , there are at most three different return times to this interval, one of them being the sum of the other two. Furthermore, two of them are always consecutive denominators in the continued fraction expression of the irrational number  $\Omega$ . This fact has also been proven for integrable Hamiltonian systems with two degrees of freedom.<sup>17</sup>

Based on Slater’s theorem, the detection of quasiperiodicity can be performed simply by counting the number of different return times that the orbit needs to recur to the neighborhood of a reference point  $\vec{v}_{\text{ref}}$ . The torus is identified with at most three different return times, which does not hold for chaotic orbits. The authors of Ref. 18 have firstly proposed to use this recurrence property to detect the existence of quasiperiodicity, which was demonstrated to be a useful and fast tool. Note that Slater’s theorem does not impose any constrictions on the size of  $\epsilon$ , provided it does not cover the whole trajectory in phase space. Therefore, for the implementation of this result, we do not have to worry about having very long recurrence times. Choosing a larger value of  $\epsilon$  we can decrease the recurrence times to the starting interval.

We use this idea and apply it to the map [Eq. (1)]. Several typical trajectories on the phase plane are shown in Fig. 1. In this plot, each orbit has a length of  $N = 2 \times 10^7$  points.<sup>24</sup> The color is encoded as follows. First, for each trajectory, we randomly choose a reference point  $\vec{v}_{\text{ref}}$  and specify a recurrence interval of  $\epsilon$  size around this point. We then count the

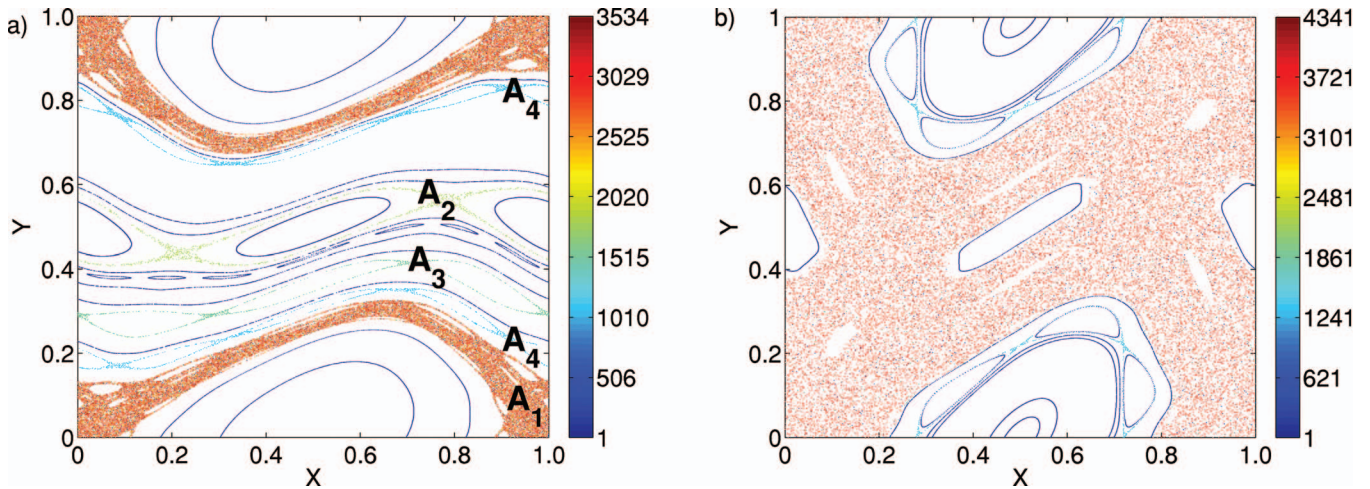


FIG. 1. (Color) The phase portrait of the standard map [Eq. (1)] with different perturbation values: (a)  $\kappa=0.8$  and (b)  $\kappa=1.4$ . The color is determined by the number of different return times. The value of 1 corresponds to periodic orbits.

number of different return times for this trajectory. Finally, we assign a color to the trajectory with respect to the number of different return times, and plot each trajectory with the associated color. In Fig. 1(a) we represent the color-coded orbits for  $\kappa=0.8$ . For  $\kappa < \kappa_{cr}=0.9716\dots$ , many rotational invariant tori are preserved while some are destroyed. When  $\kappa > \kappa_{cr}$  [Fig. 1(b),  $\kappa=1.4$ ] no rotational tori are left. In both cases, we have fixed the size of the recurrence interval to  $\epsilon=0.015$ . Trivially, periodic orbits have only one return time (darkest color). For quasiperiodic orbits (including rotational and librational circles), the number of return times is at most 3. In contrast, chaotic trajectories have a much larger number of return times (medium gray). Therefore, we see that counting the number of different return times allows classifying the type of dynamics reliably.

Another interesting property discovered by this analysis is the distinction between different stochastic layers. Taking Fig. 1(a) as an example, the chaotic region ( $A_1$ ) around the period-1 elliptic orbit, i.e.,  $(x,y)=(0.5,0)=(0.5,1)$ , has a much higher value of the number of returns, compared to the chaotic region ( $A_2$ ) around the period two elliptic orbits, i.e.,  $(0,0.5) \rightleftharpoons (0.5,0.5)$ . The same holds for the chaotic regions ( $A_3$ ) around the period-3 and -4 elliptic orbits ( $A_4$ ), as shown by gradually different colors.

From these two diagrams, one clearly observes the differences between the regular and chaotic orbits by their associated number of different return times. The predefined size of the recurrence interval  $\epsilon$  only influences the number of return times of chaotic trajectories, which increases with  $\epsilon$ . In contrast, the number of return times for regular orbits (periodic and quasiperiodic) is constant with  $\epsilon$ . Analogously, the length of the time series does not influence the number of return times for regular orbits. For chaotic orbits, the number of return times increases with the length of the trajectory. Summarizing, the number of return times for a quasiperiodic orbit is always at most 3, independently of the value of  $\epsilon$  and of the length of the trajectory. The only restriction for the value of  $\epsilon$  is that it does not cover the whole trajectory in phase space.

### III. RECURRENCE PLOTS OF ORDERED AND CHAOTIC ORBITS

As mentioned in Sec. I, the phase space of nonintegrable Hamiltonian systems is divided into subregions with regular and chaotic orbits, producing a complicated mixture of both. A typical chaotic trajectory spends a long time in the neighborhood of stable islands, showing almost regular behavior before going to the large chaotic sea. During this particular time, the orbit is stuck and is referred to as sticky orbit.<sup>5,9</sup>

In this section, we use the method of recurrence plots (RPs) to distinguish between quasiperiodic and sticky orbits in short trajectories. To illustrate our idea, we choose a sticky orbit as suggested in Ref. 5. The first 3000 iterations of the trajectory are shown in Fig. 2(b). This orbit escapes to the large chaotic area after approximate  $1.65 \times 10^5$  iterations. We call this escape time  $T_{esc}$ , which is about two orders of magnitude larger than our “observation.” In Fig. 2(a), we also plot one librational quasiperiodic orbit together with a filling chaotic one for better comparison. Based on the representations in the phase space, it is not possible to discern whether the curve of Fig. 2(b) is quasiperiodic or chaotic, since the number of iterations is much less than  $T_{esc}$ . Therefore, it is

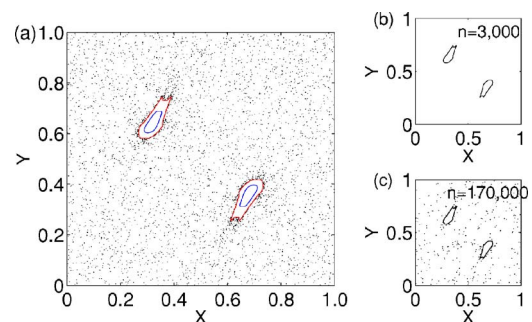


FIG. 2. (Color online) The phase portrait of the standard map for  $\kappa=5.0$ . (a) The first 3000 iterations of three orbits are plotted with different colors: quasiperiodic (gray), sticky (dark gray), and filling chaotic (black). (b) The first 3000 iterations of the sticky orbit. (c) The first  $1.7 \times 10^5$  iterations of the sticky orbit.

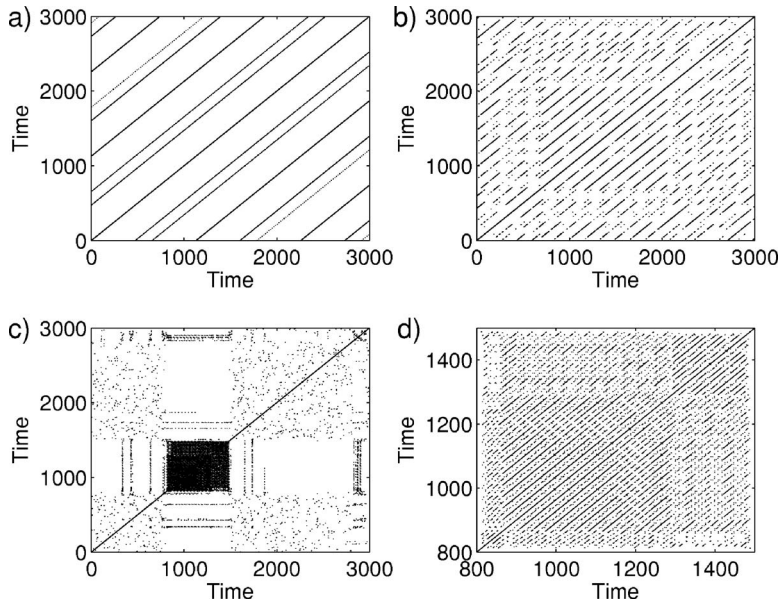


FIG. 3. RPs of different trajectories consisting of 3000 iterations. (a) quasiperiodic orbit, (b) sticky orbit, (c) filling chaotic orbit, and (d) zooming of the black structure in (c).

necessary to look at other properties of the orbit. To this end, we concentrate on the recurrence properties of the orbit.

RPs were originally introduced to visualize the recurrences of trajectories of dynamical systems in phase space.<sup>19</sup> Suppose that we have a dynamical system represented by the trajectory  $\{\vec{v}_i\}$  for  $i=1, \dots, N$  in a  $d$ -dimensional phase space. We then compute the following recurrence (binary) matrix,

$$\mathbf{R}_{i,j} = \Theta(\epsilon - \|\vec{v}_i - \vec{v}_j\|), \quad i, j = 1 \dots N, \quad (2)$$

where  $\epsilon$  is a predefined threshold,  $\Theta(\cdot)$  is the Heaviside function, and  $\|\cdot\|$  denotes a norm. The graphical representation of  $\mathbf{R}_{i,j}$ , called a “recurrence plot,” is obtained by encoding the value “1” by a black point (i.e., the distance between the respective points is smaller than the predefined threshold  $\epsilon$ ), and “0” by a white point (i.e., the distance between the respective points is larger than  $\epsilon$ ).

When calculating the recurrence matrix [Eq. (2)], a conventional way to choose  $\epsilon$  corresponding to 10% of the size of the corresponding component and the Euclidean norm are applied.<sup>20</sup> Figure 3(a) shows the RP of the quasiperiodic orbit. It consists mainly of uninterrupted diagonal lines. The number of different distances between these lines is at most 3, in accordance with Slater’s theorem. The RP of the sticky orbit exhibits a quite different feature: it consists of many dashed diagonal lines [Fig. 3(b)]. Comparing this RP to the RP of the filling orbit [Fig. 3(c)], we note that the diagonal lines of the sticky orbits are much longer, reflecting the fact that the sticky orbit is more regular than the chaotic one. The RP of the filling chaotic orbit is composed of a large number of short diagonals, which are distributed more homogeneously. The large black structure along the main diagonal of Fig. 3(c), leaving two almost blank bands in the vertical and horizontal directions, is due to the presence of the stable islands. When the chaotic trajectory visits the neighborhood of one stable island, the dynamics is again stuck for some time [Fig. 3(d)]. We notice a relatively “weak” sticky behavior compared to the “strong” stickiness of Fig. 3(b) within

our observation time. Note that stickiness is a general property of a chaotic orbit in Hamiltonian systems.

From the above RP representations, it is rather straightforward to see the differences between them, showing that RPs are a powerful tool for the characterization of the dynamics. Note that it is possible to distinguish between quasiperiodic and sticky orbits even in much shorter trajectories than 3000 iterations. Using Slater’s theorem, it is possible to detect the existence of quasiperiodicity in only ten orbital periods with about 700 points.<sup>21</sup>

An alternative method to distinguish quasiperiodic from chaotic orbit is based on stretching numbers. The calculation of the spectrum of stretching numbers proposed by Contopoulos *et al.*<sup>4,5</sup> consists of two steps. First, one specifies an infinitesimal deviation from the initial condition to compute the stretching numbers, which only works in the case that the equations are known. The second step is to construct the spectrum taking care of the bin size and the number of bins. In order to obtain a reliable spectrum, at least  $10^3$ – $10^4$  points are required.<sup>6</sup> This is computationally more complicated than the RPs we propose here, which are simple and numerically convenient. We only consider the distance between any two points of the trajectory and encode the recurrence matrix into a two-dimensional plot.

#### IV. RECURRENCE QUANTIFICATION ANALYSIS OF THE STICKINESS

In order to quantify the patterns in the RPs, several measures are commonly used, which are part of the recurrence quantification analysis (RQA).<sup>20</sup> Here, we apply three measures:

- Recurrence rate (RR), defined as the percentage of black points in the RP, i.e.,

$$\text{RR} = \frac{1}{N^2} \sum_{i,j=1}^N \Theta(\epsilon - \|\vec{v}_i - \vec{v}_j\|). \quad (3)$$

TABLE I. Three selected RP-based measures of complexity computed from trajectories shown in Figs. 3(a)–3(c) ( $l_{\min}=2$ ).

$\epsilon=0.025$	RR	DET	$L_{\text{mean}}$
Quasiperiodic	0.131	0.67	25.80
Sticky	0.074	0.68	12.99
Filling chaotic	0.006	0.64	5.12

- Determinism (DET), defined as the percentage of black points belonging to a diagonal line of at least length  $l_{\min}$ ,

$$\text{DET} = \frac{\sum_{l=l_{\min}}^N IP(l)}{\sum_{l=1}^N IP(l)}, \tag{4}$$

where  $P(l)$  denoted the probability to find a diagonal line of length  $l$  in the RP. However, this measure does not have the real meaning of the determinism of the process. This measure aims to quantify how predictable a system is.

- Average diagonal line length ( $L_{\text{mean}}$ ), defined as

$$L_{\text{mean}} = \frac{\sum_{l=l_{\min}}^N lP(l)}{\sum_{l=l_{\min}}^N P(l)} \tag{5}$$

is the average time that two segments of the trajectory are close to each other, and can be interpreted as the mean prediction time.

Up to now, more than ten different measures are commonly used to quantify the structures in an RP. For an exhaustive overview of other measures and associated applications in data analysis, see Ref. 20. For this study, we calculated all other RQA measures and found results similar to those presented in this paper.

The values of the three measures computed from the first 3000 iterations of each trajectory (quasiperiodic, sticky, and chaotic) are summarized in Table I. We observe that RR and  $L_{\text{mean}}$  distinguish very clearly between the different orbits. The only measure that does not perform sufficiently well is DET, which is probably due to the ambiguity by choosing  $l_{\min}$ .<sup>20</sup>

In order to compare the recurrence based method with other standard techniques, we calculate the Lyapunov exponents ( $\lambda_{\text{max}}$ ), which are dependent on the iteration time for the three orbits (Fig. 4). From this figure, we see that on short time scales (i.e., time series with a length less than  $10^5$ ),  $\lambda_{\text{max}}$  is not able to distinguish between sticky and quasiperiodic orbits. In the present case,  $\lambda_{\text{max}}$  works only if the

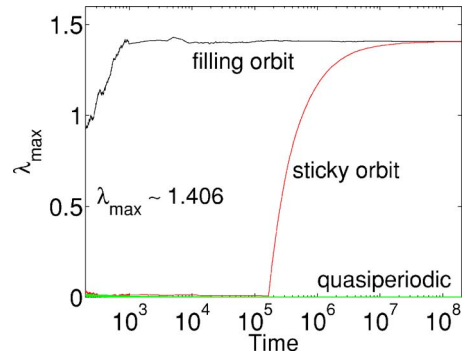


FIG. 4. (Color online) Lyapunov exponents for three orbits with a dependence on the iteration time. Since the initial conditions for the sticky and filling orbits are in the same chaotic component,  $\lambda_{\text{max}}$  converge to the same value of 1.406, albeit after a long time.

length of the time series is much larger than  $10^5$  (i.e., no less than  $10^8$ ). In contrast, the method of RPs is able to characterize the dynamics from very short time series (3000 data points), both visually (Fig. 3) and quantitatively (Table I).

Furthermore, following the sticky orbit for a long time (e.g.,  $N=3 \times 10^5$ ), the RQA measures are able to capture the dynamical transition of the trajectory. Due to the large number of points of the orbit, we analyze it by applying the RQA measures in moving windows of length  $w$  (Fig. 5). The size of each window is  $w=5000$  points and there are 4500 points overlapped between two consecutive windows. Hence, the measures defined above correspond to a respective running window:  $RR_i$ ,  $DET_i$  and  $L_{\text{mean}i}$ ,  $i=1, \dots, 600$ . In Fig. 5, the selected RQA measures are monitored with a dependence on time. These measures capture the transition time  $T_{\text{esc}}$  reasonably; e.g., DET decreases suddenly at the transition point because the trajectory becomes more irregular. Note that the additional parameter  $w$  can be chosen rather arbitrary as long as sufficient recurrences are obtained within a window.

Another way to visualize long sticky orbits is to apply the windowed and meta-recurrence plots.<sup>22</sup> The meta-RPs are obtained by covering an RP with  $w \times w$ -sized squares and by averaging the recurrence points contained in each window. Consequently, a windowed recurrence plot is an  $N_w \times N_w$  matrix, where  $N_w$  is the floor-rounded  $N/w$  and consists of values not limited to 0 and 1, which suggests a color-encoded representation. These values correspond to the cross correlation sum

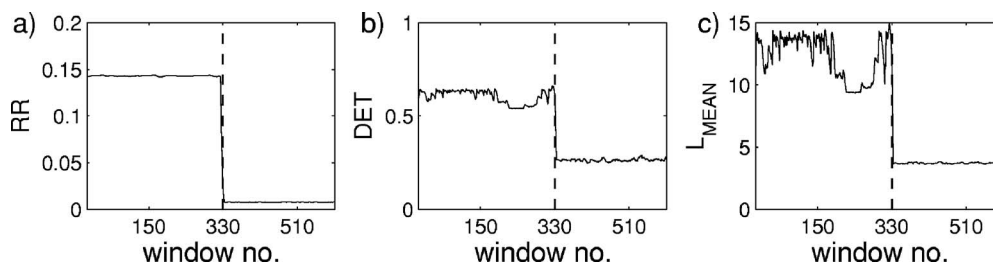


FIG. 5. RQA measures with a dependence on time for the sticky orbit. The size of each window is  $w=5000$  points and there are 4500 points overlapped between two consecutive windows. The vertical dashed line corresponds to the transition time around  $1.65 \times 10^5$ . The length of the orbit is  $N=3 \times 10^5$  points.

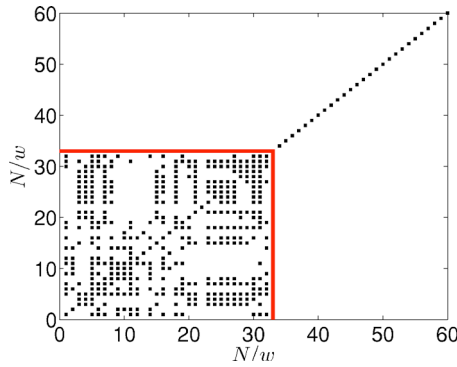


FIG. 6. (Color online) Thresholded meta-recurrence plot of the sticky orbit. There exists a significant change in the density at the transition point denoted by the solid lines. The window size  $w=5000$ .

$$C(\epsilon, I, J) = \frac{1}{w^2} \sum_{i=1+(I-1)w}^{I_w} \sum_{j=1+(J-1)w}^{J_w} \Theta(\epsilon - \|\vec{v}_i - \vec{v}_j\|), \tag{6}$$

$$I, J = 1 \cdots \frac{N}{w}.$$

The meta-RP has been defined as a distance matrix derived from the cross-correlation sum [Eq. (6)]:

$$D(\epsilon, I, J) = \frac{1}{\epsilon^2} (C(\epsilon, I, I) + C(\epsilon, J, J) - 2C(\epsilon, I, J)). \tag{7}$$

By applying a further threshold to  $D(\epsilon, I, J)$ , a black-white dotted representation is also possible. These modified RPs were successfully used to characterize nonstationarity in time series.<sup>22</sup> Furthermore, meta-recurrence plots correspond to a zooming-out version of the normal RPs. These modified RPs help to shorten the computation time significantly, at least of the order of  $N$  even for a naive configuration.<sup>22</sup> The most important advantage of meta-RPs is that they make the visualization of long data sets possible. In Fig. 6, the thresholded meta-RP of a sticky orbit is represented. There is a dramatic change in the density of recurrence points at the time when the trajectory leaves the sticky region for the chaotic sea. The transition point is clearly visible (solid lines) in the plot.

As we see from Table I and Fig. 5(a), RR is much higher for sticky orbit comparing to filling orbit. This is due to the fact that the trajectory is confined to a rather small subset of the phase space. This is related to the mean recurrence time

$$\langle T \rangle = \int_0^\infty TP(T)dT = \frac{1}{\mu(I)}, \tag{8}$$

where  $P(T)$  is the distribution of the recurrence times  $\{T_1, T_2, \dots, T_M, \dots\}$  of the orbit to a predefined recurrence region and  $\mu(I)$  is to the measure of this recurrence region. This is the so-called Kac’s lemma.<sup>23</sup> For the numerics, the integral should be replaced by a sum. As we mentioned in Sec. I, a typical recurrence time distribution  $P(T)$  of a chaotic orbit in a Hamiltonian system shows an exponential decay for short times related to the events that do not stick, followed by a power-law decay for large times attributed to the stickiness. The exponent is proportional to the mean recurrence time  $\langle T \rangle$  of Eq. (8). When the trajectory is not stuck, one expects a large value of  $\langle T \rangle$  as it has an exponential decay. On the contrary, smaller  $\langle T \rangle$  is observed on the time scales when it is stuck. The trajectory shows a slower divergence (power-law decay) in the “sticking” window. In terms of RR, for this particular window,  $w_i$ , more black points are obtained, leading to a higher value of RR. Furthermore, the slow divergence is reflected by relatively longer diagonal lines in the RPs. As a consequence, the value of DET is also higher during the sticking events.

### V. QUANTIFICATION OF STICKINESS BY RP

During its evolution in time, a typical chaotic orbit visits the neighborhood of the stable islands from time to time. Next, we study the stickiness in a more general framework by means of one measure of RQA; namely, RR. The calculations based on other RQA measures can be performed in a similar way.

We use again the standard map [Eq. (1)] with  $\kappa=1.5$ . The variation of  $RR_i, i=1, \dots, N/w$ , in running windows of length  $w$  is monitored. Figure 7 illustrates a typical chaotic orbit and its associated variation of RR, dependent on time. When the trajectory is trapped in a sticky region, the RR

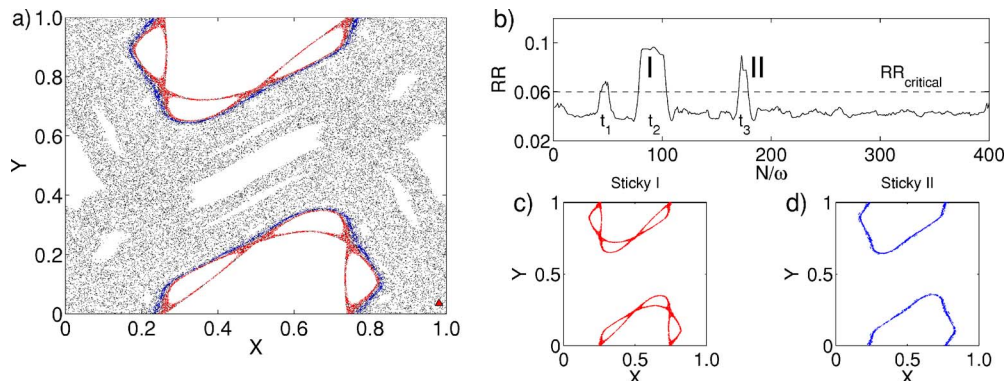


FIG. 7. (Color online) (a) The phase portrait of the parameter  $\kappa=1.5$  with initial values indicated by the black upward triangle point for  $2 \times 10^5$  iterations. Sticky regions I and II are colored with medium gray and dark gray, respectively. (b) Dependence of the RR with a running window of size  $w=5000$  with 4500 points overlapped between two consecutive windows. The small peak at  $\approx 45$  is due to weaker stickiness in comparison with I and II. The series of the sticking events is denoted by  $\{t_1, t_2, t_3, \dots\}$ . (c, d) Two major sticky regions in the phase plane.

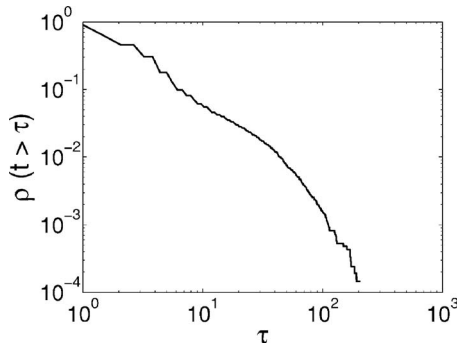


FIG. 8. Cumulative distribution of sticking events of duration  $t$  greater than  $\tau$ . A single chaotic trajectory consisting of  $10^9$  iterations has been used for the computation.

shows a significant change due to the regular evolution in this particular time interval. As Fig. 7(b) indicates, two major sticky time epochs are obtained corresponding to two sticky regions, denoted as “I” and “II.” In the bottom panels [Figs. 7(c) and 7(d)], the corresponding trajectories are shown for comparison. Furthermore, one finds that a small proportion of sticking time occurs at the window number  $\approx 45$ , indicating that the trajectory is stuck for a smaller time compared to the regions I and II. In what follows, we only consider the sticking events without the specifications of the location of the sticky regions. It is not necessary to do so, since there are many different stable islands in phase space.

From the variation of RR with time, the sticking events are identified by those regimes where RR is larger than  $RR_{cr}$  [Fig. 7(b)]. Here,  $RR_{cr}$  is chosen to be 5% higher than the overall average level when the trajectory is not stuck. However, the choice of  $RR_{cr}$  is not crucial, as the value of RR for the sticking events is much higher than the value for the events they do not stick. Hence, based on Fig. 7(b), we obtain a series  $\{t_1, t_2, t_3, \dots, t_i, \dots, \infty\}$  with  $t_i$  denoting the duration of the  $i$ th sticking event. The duration of the  $i$ th sticking event is then the time interval  $t_i = w\Delta_i$  between the  $i$ th and  $(i + \Delta_i)$ th windows satisfying  $\prod_{m=1}^{\Delta_i} \Theta(RR_{i+m} - RR_{cr}) = 1$ . We can now consider the probability to find a sticking event which has a time span  $t > \tau$ , namely, by the calculation of the following cumulative distribution:

$$\rho(t > \tau) = \sum_{t=\tau}^{\infty} P(t). \quad (9)$$

This cumulative distribution is shown in Fig. 8, indicating a power-law decay  $\rho(t > \tau) \sim \tau^{-\gamma}$  with  $\gamma \approx 1.924$ . This result is in good agreement with the results from the recurrence time statistics analysis presented in Refs. 11 and 15.

## VI. CONCLUSIONS

We have used the method of recurrence plots (RPs) to characterize the stickiness in nonintegrable Hamiltonian systems. This approach enables distinguishing clearly between regular (periodic and quasiperiodic) and chaotic orbits from very short trajectories. Slater’s theorem guarantees at most three different return times for a quasiperiodic orbit to come back to a predefined recurrence interval. The persistence of

this number in integrable Hamiltonian systems with two degrees of freedom allows us to divide the phase space into regular and chaotic subregions rather easily. The RPs of chaotic orbits during the sticking time are substantially different from the RPs of quasiperiodic trajectories.

Furthermore, measures from the recurrence quantification analysis (RQA) characterize the complex patterns in the RPs, allowing the distinction between chaotic orbits that are temporarily trapped in a sticky domain and quasiperiodic orbits from very short trajectories. Based on these RQA measures, the dynamical transitions from sticky regions to the large chaotic sea are also captured. Following a single chaotic trajectory, we have found an asymptotic power-law decay of the cumulative distribution of the duration of sticking events, in accordance with results reported in the literature.<sup>11,15</sup>

In the present work, we have used the standard map as a representative example of a system showing stickiness. The extension to higher dimensional systems by RPs analysis needs further study. Nevertheless, in higher dimensional cases RPs would also work to distinguish ordered from chaotic orbits because there is no dimensionality limitation in the recurrence matrix [Eq. (2)]. This method could have applications in many fields, such as astrophysics, where the characterization of regular and chaotic orbits is of great relevance.<sup>4</sup>

## ACKNOWLEDGMENTS

The authors would like to thank Diego Pazó for very fruitful discussions. This work was supported by the International Helmholtz Institute for Super-computational Physics (MWFK Land Brandenburg), SPP 1114 (DFG), and the Promotionskolleg Behavioral and Cognitive Dynamics (Excellence Programme, Potsdam University). The constructive and careful comments and suggestions from the referees are also acknowledged.

<sup>1</sup>A. Lichtenberg and M. Leiberman, *Regular and Chaotic Dynamics*, 2nd ed. (Springer, Berlin, 1992).

<sup>2</sup>D. K. Umberger and J. D. Farmer, *Phys. Rev. Lett.* **55**, 661 (1985).

<sup>3</sup>H. Kantz and P. Grassberger, *Phys. Lett. A* **123**, 437 (1987).

<sup>4</sup>G. Contopoulos, *Order and Chaos in Dynamical Astronomy* (Springer, New York, 2004).

<sup>5</sup>G. Contopoulos, N. Voglis, and R. Dvorak, *Celest. Mech. Dyn. Astron.* **67**, 293 (1997).

<sup>6</sup>G. Contopoulos, *Ann. N.Y. Acad. Sci.* **867**, 14 (1998).

<sup>7</sup>C. F. F. Karney, *Physica D* **8**, 360 (1983).

<sup>8</sup>J. D. Meiss and E. Ott, *Phys. Rev. Lett.* **55**, 2741 (1985).

<sup>9</sup>H. E. Kandrup, C. Siopis, G. Contopoulos, and R. Dvorak, *Chaos* **9**, 381 (1999).

<sup>10</sup>J. Meiss, *Rev. Mod. Phys.* **64**, 795 (1992).

<sup>11</sup>G. Zaslavsky, *Phys. Rep.* **371**, 461 (2002).

<sup>12</sup>R. Artuso and A. Prampolini, *Phys. Lett. A* **246**, 407 (1998).

<sup>13</sup>E. G. Altmann, A. E. Motter, and H. Kantz, *Phys. Rev. E* **73**, 026207 (2006).

<sup>14</sup>G. Contopoulos, *Astron. J.* **76**, 147 (1971).

<sup>15</sup>B. V. Chirikov and D. L. Shepelyansky, *Physica D* **13**, 395 (1984).

<sup>16</sup>N. Slater, *Proc. Cambridge Philos. Soc.* **63**, 1115 (1967).

<sup>17</sup>D. Mayer, *Lett. Math. Phys.* **16**, 139 (1988).

<sup>18</sup>E. G. Altmann, G. Cristadoro, and D. Pazó, *Phys. Rev. E* **73**, 056201 (2006).

<sup>19</sup>J.-P. Eckmann, S. Kamphorst, and D. Ruelle, *Europhys. Lett.* **4**, 973 (1987).

<sup>20</sup>N. Marwan, M. Romano, M. Thiel, and J. Kurths, *Phys. Rep.* **438**, 237 (2007).

<sup>21</sup>Y. Zou, D. Pazo, M. C. Romano, M. Thiel, and J. Kurths, *Phys. Rev. E* **76**, 016210 (2007).

<sup>22</sup>M. Casdagli, *Physica D* **108**, 12 (1997).

<sup>23</sup>M. Kac, *Probability and Related Topics in Physical Sciences* (Interscience, New York, 1959).

<sup>24</sup>In our computations, 500 initial values are chosen randomly. From these trajectories several typical orbits are represented to be computer memory efficient. If we did not proceed so, a figure like Fig. 1(a) would require approximately 15 GB of hard-disk space. There are no trajectories in the white regions of Fig. 1 for the initial values we choose, which are excluded from the color bar.